Special Aspects of Composed Kinetic-Hydrodynamic Model When Describing the Shape of Shockwaves

YU.A.NIKITCHENKO, S.A.POPOV, A.V.TIKHONOVETS
Aerodynamics department
Moscow Aviation Institute (National Researching University)
125993, Moscow, Volokolamskoe shosse, 4
RUSSIAN FEDERATION
nikitchenko7@ya.ru, flowmech@mail.ru, tikhalena@gmail.com, www.mai.ru

Abstract: A mathematical model of the flow of a polyatomic gas containing a combination of the Navier-Stokes-Fourier model (NSF) and the model kinetic equation of polyatomic gases is presented. At the heart of the composed components is a unified physical model, as a result of which the NSF model is a strict first approximation of the model kinetic equation. The model allows calculations of flow fields in a wide range of Knudsen numbers (Kn), as well as fields containing regions of high dynamic nonequilibrium. The boundary conditions on a solid surface are set at the kinetic level, which allows, in particular, to formulate the boundary conditions on the surfaces absorbing or emitting gas. The composed model was tested. The example of the problem of the shock wave profile shows that up to Mach numbers $M \approx 2$ the combined model gives smooth solutions even in those cases where the sewing point is in a high gradient region. For the Couette flow, smooth solutions are obtained at $M = 5$, $Kn = 0.2$. As a result of research, a weak and insignificant difference between the kinetic region of the composed model and the "pure" kinetic model was established. A model effect was discovered: in the region of high nonequilibrium, there is an almost complete coincidence of the solutions of the kinetic region of the combined model and the "pure" kinetic solution.
This work was conducted with the financial support of the Ministry of Education and Science of the Russian Federation, project №9.7170.2017/8.9.

Key-Words: polyatomic gases, Navier-Stokes-Fourier model, model kinetic equation, composed model, dynamic nonequilibrium, sorption surfaces.

1 Introduction

Modern aerospace and nanotechnologies are in need of the improved computational methods and mathematical models of gas flow in a wide range of Mach and Knudsen numbers. One of the areas to which the present paper belongs is related to the development of hybrid or composed flow models. These models involve the combined use of the methods of molecular kinetic theory and continuum mechanics.

A number of models include the separation of the computational domain of geometric space into hydrodynamic and kinetic subdomains, for example [1, 2, 3]. In the hydrodynamic subdomain, the Navier-Stokes equations are used; in the kinetic subdomain, the BGK model kinetic equation with a certain numerical implementation, or statistical models, are used.

The models of [4, 5] distinguish hydrodynamic and kinetic subdomain in the velocity space: hydrodynamic subdomain for "slow" molecules and kinetic subdomain for "fast" molecules. In the subdomain of "slow" molecules, the Euler or Navier-Stokes models are used, and in the subdomain of "fast" molecules the BGK equation is used.

The BGK model was obtained for the weight function (the velocity distribution function of molecules) of a monatomic gas. Its collision integral corresponds to a gas with a Prandtl number $Pr = 1$ [6]. Thus, this model implies some hypothetical gas. The continuous transition from this model to hydrodynamic is very difficult without the use of artificial smoothing procedures [1].

The model [7] in the kinetic subdomain of the geometric space uses the S-model [6], which distinguishes it favorably from the models cited above. When calculating the flow near a rough surface, satisfactory results were obtained even in the transition region of the flow. The limitation of this model lies in the fact that the consistency of the kinetic and hydrodynamic description exists only for monatomic gases.

The present work has as its goal the development of a composed model of the flow of polyatomic gases. The Navier-Stokes-Fourier model (NSF) [8] is composed with the model kinetic equation of polyatomic gases (MKE) [9]. The NSF model is a rigorous first approximation of the system of moment equations for polyatomic gases [10]. When obtaining this approximation, nonequilibrium quantities (stress deviator, heat fluxes, difference of translational and rotational temperatures) in their moment equations were set so small that their second and higher degrees can be neglected. Flows that satisfy the conditions of the first approximation will be called weakly nonequilibrium.

The relaxation terms of MKE are obtained using the polyatomic gas system used in the development of the NSF model. The coefficient of bulk viscosity of the NSF model is presented in such a way that this model is the first approximation in the above sense of the MKE model. Thus, both composable models are based on a single physical model.

As a result of research, a weak and insignificant difference between the kinetic region of the composed model and the "pure" kinetic model was established. A model effect was discovered: in the region of high nonequilibrium, there is an almost complete coincidence of the solutions of the kinetic region of the combined model and the "pure" kinetic solution.

This paper focuses primarily on solving practical problems. In this regard, there is no review of an extensive range of works with a theoretical orientation.

2 Basic Assumptions and Notations

We consider the flow of monocomponent perfect gases. All expressions are written for polyatomic gases. In the case of monatomic gases, the expressions remain valid after obvious transformations.

The index writing of tensor expressions is used. A repeated Greek index indicates a summation from 1 to 3.

The velocity space integral is denoted by $\int \dots d\mathbf{c} \equiv \int_{-\infty}^{+\infty} dc_1 \int_{-\infty}^{+\infty} dc_2 \int_{-\infty}^{+\infty} \dots dc_3$

The notations used are:

δ_{ij} – Kronecker delta;

t, x_i, ξ_i – time, geometric coordinate and molecular velocity;

m_0, n, $\rho = m_0 n$ – molecular mass, molecular concentration and gas density;

u_i, $c_i = \xi_i - u_i$ – group (macroscopic) and thermal molecular velocities;

f – weight function (molecular velocity distribution function);

c_p, c_v, γ, k, $R = k/m_0$ – heat capacities at constant pressure and volume, specific heat ratio, Boltzmann constant, specific gas constant;

T_t, T_r, $T = 1.5(\gamma-1)T_t + 0.5(5-3\gamma)T_r$ – temperatures of translational and rotational degrees of freedom of molecules, thermodynamic temperature;

P_{ij}, $p_{ij} = P_{ij} - \delta_{ij} R\rho T_t$ – total and nonequilibrium stresses;

$p = P_{\alpha\alpha}/3 = R\rho T_t$ – mechanical pressure;

φ_i, ω_i – heat fluxes caused by the transport of energy of thermal motion on the translational and rotational degrees of freedom of molecules;

$q_i = \varphi_i + \omega_i$ – full heat flux;

M, Kn, Pr – Mach, Knudsen and Prandtl numbers.

In considered models it is accepted: $Pr = 4\gamma/(9\gamma - 5)$.

3 Composed Model

3.1 Hydrodynamic model

The NSF model, which differs from the traditional system of conservation equations in the Navier-Stokes approximation by the presence of the coefficient of bulk viscosity in the equations of nonequilibrium stress, is considered as a hydrodynamic model. In terms of [8], the system of equations of this model has the following form:

$$\begin{cases} \dfrac{\partial \rho}{\partial t} + \dfrac{\partial \rho u_\alpha}{\partial x_\alpha} = 0 \\ \dfrac{\partial u_i}{\partial t} + u_\alpha \dfrac{\partial u_i}{\partial x_\alpha} + \dfrac{1}{\rho}\dfrac{\partial P_{i\alpha}}{\partial x_\alpha} = 0 \qquad i = 1,2,3 \\ \dfrac{\partial T}{\partial t} + u_\alpha \dfrac{\partial T}{\partial x_\alpha} + (\gamma-1)\dfrac{P_{\alpha\beta}}{\rho}\dfrac{\partial u_\alpha}{\partial x_\beta} + \dfrac{1}{c_v \rho}\dfrac{\partial q_\alpha}{\partial x_\alpha} = 0 \end{cases} \quad (1)$$

where

$$P_{ij} = \delta_{ij} R\rho T - \mu\left(\frac{\partial u_i}{\partial x_j} + \frac{\partial u_j}{\partial x_i}\right) + \delta_{ij}\frac{2}{3}\left(1 - \frac{5-3\gamma}{2}Z\right)\mu\frac{\partial u_\alpha}{\partial x_\alpha}$$

$$q_i = -\frac{c_p}{\mathrm{Pr}}\mu\frac{\partial T}{\partial x_i}$$

We specifically note that in the definition of the molecular-kinetic theory, in contrast to continuum mechanics, normal stresses are positively defined quantities, see (5). For the compatibility of the kinetic MKE model and the hydrodynamic NSF model in the system (1), the stress tensor is written in the molecular-kinetic interpretation.

The viscosity coefficient μ and the parameter Z are determined by the dependencies [12, 16], which are used in the MKE model, but with preservation of the order of approximation of the NSF model, i.e. $\mu = \mu(T_t = T)$, $Z = Z(T_t / T_r = 1)$. In [8] it was shown that the coefficient of bulk viscosity allows expressing temperatures T_t and T_r in terms of temperature T in the hydrodynamic approximation; however, in the region of highly nonequilibrium flows, this approximation gives qualitatively incorrect results.

3.1 Kinetic model

As a kinetic model of the flow, the MKE model [9] is used, built for a single-particle weight function, the phase space of which is supplemented by the energy of rotational degrees of freedom ε: $f(t, \mathbf{x}, \boldsymbol{\xi}, \varepsilon)$. After reducing the dimension of the weight function, the kinetic equations of the model take the form:

$$\frac{\partial}{\partial t}\begin{vmatrix} f_t \\ f_r \end{vmatrix} + \xi_\alpha \frac{\partial}{\partial x_\alpha}\begin{vmatrix} f_t \\ f_r \end{vmatrix} = \frac{p}{\mu}\begin{vmatrix} f_t^+ - f_t \\ f_r^+ - f_r \end{vmatrix}, \qquad (2)$$

where

$$f_t = \int f d\varepsilon,\ f_r = \int \varepsilon f d\varepsilon,$$

$$f_t^+ = \frac{n}{\left(2\pi R T_t^+\right)^{3/2}} \exp\left(-\frac{c^2}{2RT_t^+}\right)\left(1 + \frac{\varphi_\alpha c_\alpha}{3\rho\left(RT_t^+\right)^2}\left(\frac{c^2}{5RT_t^+} - 1\right)\right)$$

$$f_r^+ = \frac{5-3\gamma}{2(\gamma-1)} k T_r^+ f_t^+,$$

$$T_t^+ = T + 0.5(5-3\gamma)(1-1/Z)(T_t - T_r),$$

$$T_r^+ = T - 1.5(\gamma-1)(1-1/Z)(T_t - T_r),$$

$$T_t = (3Rn)^{-1}\int c^2 f_t d\mathbf{c}$$

$$T_r = 2(\gamma-1)\left((5-3\gamma)R\rho\right)^{-1}\int f_r d\mathbf{c},$$

$$\varphi_i = 0.5 m_0 \int c_i c^2 f_t d\mathbf{c}$$

The viscosity coefficient $\mu = \mu(T_t)$ and the parameter $Z = Z(T_t, T_r)$ showing the amount of intermolecular collisions per one inelastic collision are considered as free parameters of the model.

The remaining moments of the weight function required for the composed model are defined as:

$$n = \int f_t d\mathbf{c}, \qquad (3)$$

$$u_i = n^{-1}\int \xi_i f_t d\mathbf{c}, \qquad (4)$$

$$P_{ij} = m_0 \int c_i c_j f_t d\mathbf{c}, \qquad (5)$$

$$\omega_i = \int c_i f_r d\mathbf{c}. \qquad (6)$$

In [9], the results of calculations using MKE were compared with the well-studied R-model [11, 12] and experimental data [13, 14]. Fig. 1 demonstrates a satisfactory agreement between the calculated profile of a plane hypersonic shock wave and experimental data even for such a "thin" parameter as the temperature of the rotational degrees of freedom. In the test calculations of this work, the MKE model that is not composed with the hydrodynamic model is considered as a reference.

It should be noted that the models are well consistent, since the NSF model is a strong first approximation of the kinetic model.

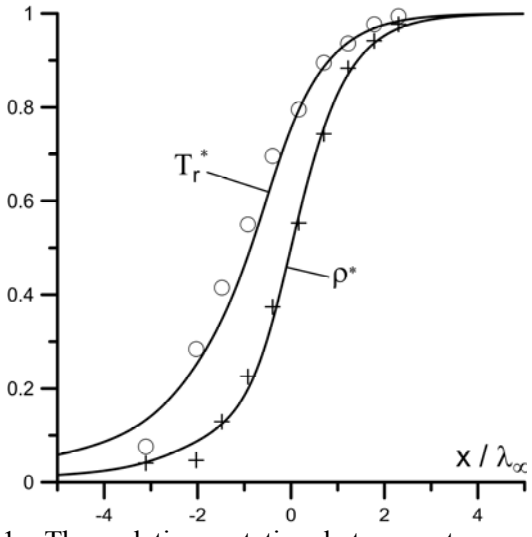

Fig. 1. The relative rotational temperature and density profiles. Model Kinetic Equation (MKE). Gas – nitrogen. $M_\infty = 7$. ○ and + – experimental data [14]

4 The Method of Composing Kinetic and Hydrodynamic Models

One of the applications of the composed model involves the application of the kinetic model in strongly nonequilibrium domains of the flow field and the hydrodynamic model in other domains.

Another application relates to weakly nonequilibrium flows near active (gas-absorbing or gas-emitting) surfaces. In this case, the kinetic model is necessary only for the formation of

boundary conditions on the surface. In Fig. 2. the schemes of the computational domain for both cases are presented: variants A and B, respectively. The vertical line on variant B denotes a streamlined surface.

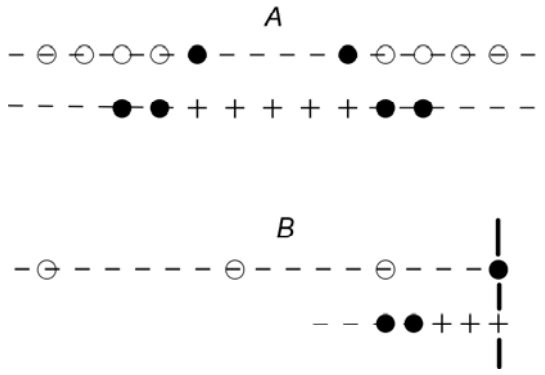

Fig.2. Schemes of computational domains. ○ – nodes of the hydrodynamic model, + – nodes of the kinetic model, ● – models joining nodes

Without loss of generality, we consider a one-dimensional stationary flow field with a geometrical coordinate $x_i \equiv x$, and a velocity coordinate corresponding to it. It is supposed that a finite-difference method is used for a numerical solution. Derivatives in system (1) are approximated by central differences on three nodes, in system (2) by one-sided differences upstream, also on three nodes. Note that the direction of flow in the kinetic equations is determined by the direction of the molecular velocity. In this case, it is a speed ξ_x that has two opposite directions. Consequently, there are two multidirectional difference schemes. Such a discrete analogue of the computational domain will later be used for numerical tests. Here it is given only for clarity of presentation and is not of fundamental importance.

In both variants on Fig. 2, the computational domain is shown twice, separately for the hydrodynamic (open circles) and kinetic (cross) models. In option A, the solution area of the hydrodynamic solution is divided into two subdomains. The boundary conditions of the left subdomain are formed in the node (the joining node), indicated by a black dot and belonging to the area of the kinetic solution. For the selected differential template, one node is sufficient. Values ρ, u_x, T in this node are defined as the moments of the weight function calculated in the kinetic domain. Similar is the solution in the right subdomain of the hydrodynamic solution. When describing a flow in the near-wall region, one hydrodynamic subdomain is sufficient. In variant A, a kinetic subdomain is located between the hydrodynamic subdomain and the wall (not shown in Fig. 2).

The boundary conditions of the kinetic solution are formed in the nodes of the hydrodynamic domain (black circles): two nodes in each hydrodynamic subdomain for the corresponding ($\xi_x > 0$ or $\xi_x < 0$) difference patterns. Since the hydrodynamic model is less informative than the kinetic model, an approximating weight function is used to reconstruct the weight function in the nodes. In the case of a near-wall flow, the weight function is determined in the node boundary with the wall, which is determined by the law of interaction of molecules with a solid surface.

Taking into account the order of approximation of the hydrodynamic model, as an approximating weight function, it is advisable to take the expansion of the equilibrium, Maxwell function. Such an expansion is used in a number of works, for example [7], for monatomic gases. In the case of polyatomic gas for functions f_{At} и f_{Ar} similar expansions lead to the expressions [9]:

$$f_{At} = f_M\left(1+\frac{1}{\rho\left(RT_t\right)^2}\left(\frac{1}{2}p_{\alpha\beta}c_\alpha c_\beta+\varphi_\alpha\left(\frac{c^2}{5RT_t}-1\right)c_\alpha\right)\right) \quad (7)$$

$$f_{Ar} = kT_r\left(\frac{5-3\gamma}{2(\gamma-1)}f_{At}+f_M\frac{\omega_\alpha c_\alpha}{\rho R^2 T_t\, T_r}\right), \quad (8)$$

$$f_M = \frac{n}{\left(2\pi RT_t\right)^{3/2}}\exp\left(-\frac{c^2}{2RT_t}\right). \quad (9)$$

The macroparameters of these expressions are determined by the hydrodynamic model and are considered in the appropriate approximation:

$T_t = T_r = T$,

$$p_{ij} = -\mu\left(\frac{\partial u_i}{\partial x_j}+\frac{\partial u_j}{\partial x_i}\right)+\delta_{ij}\frac{2}{3}\left(1-\frac{5-3\gamma}{2}Z\right)\mu\frac{\partial u_\alpha}{\partial x_\alpha},$$

$$\varphi_i = -\frac{15}{4}R\mu\frac{\partial T}{\partial x_i}, \qquad \omega_i = -\frac{5-3\gamma}{2(\gamma-1)}R\mu\frac{\partial T}{\partial x_i}.$$

Variant B in Fig. 2 assumes a solution of the NSF model in the entire computational domain. This allows to build computational grids with hydrodynamic steps, which is fundamentally important for small Kn. The grid of the kinetic solution with a step of the order of the mean free path of the molecules is constructed within the last, near-wall step of the hydrodynamic grid. Macroparameters, ρ, u_x, T, in the joining nodes are obtained by interpolating the hydrodynamic solution.

After calculating the weight function of molecules moving to the surface, the weight function of the reflected molecules is restored at the boundary node. For this, any law of interaction of molecules with the surface is used. For example, for chemo or cryosorbing surfaces, the diffuse reflection law can be used, taking into account the mass absorption coefficient [15].
At the next stage, the weight function of the reflected molecules is calculated and macroparameters are calculated in the kinetic domain. For the general, hydrodynamic solution, only the boundary node macroparameters are used. The kinetic model is used only to form the boundary conditions of the hydrodynamic model.

5 Numerical Tests

5.1 Couette Plane Flow

Numerical tests of the composed model (variant A) using the example of the Couette flow are described in [18]. In this work, the main features of the model when used in the near-wall region of the flow are noted and variants A and B are compared. In contrast to the general flow pattern (Fig. 2), variant A contains only one hydrodynamic subdomain in this problem. One of the boundaries of the kinetic subdomain is located on a streamlined surface. At this boundary, the weight function of the reflected molecules is restored in accordance with the adopted law of interaction of molecules with the surface.
The flow pattern and the applied coordinate system are shown in Fig. 3

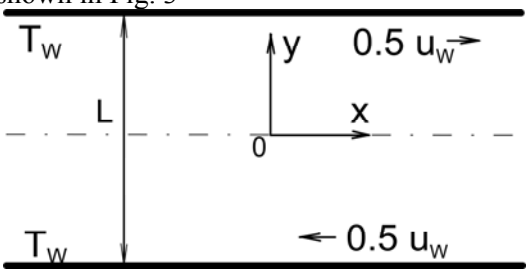

Fig.3. Couette flow pattern.
The characteristic path length of the molecule, the Mach and Knudsen numbers are defined as

$$\lambda_0 = 3.2\mu_0\left(2\pi RT_w\right)^{-1/2}/\rho_0 \qquad (10)$$

$$\mathrm{M} = u_w/\sqrt{\gamma RT_w}\,, \qquad (11)$$

$$\mathrm{Kn} = \mu_0\left(\rho_0 L\sqrt{RT_w}\right)^{-1}. \qquad (12)$$

Here ρ_0 is the gas density before the plates start moving, μ_0 is the viscosity coefficient calculated from the plate temperature.

The system of equations of the MKE model corresponds to (11) with the replacement of the index x by y. On the surface of the plates for this model, the diffuse law of reflection of molecules with the energy accommodation coefficient equal to unity is adopted.
The system of equations (1) of the NSF model is transformed as follows. The equations of mass conservation turn into a trivial identity. The density field is determined by the momentum conservation equation written for u_y. In the stationary flow $u_y = 0$ and the law of conservation of momentum is reduced to

$$\partial P_{yy}/\partial y = 0\,. \qquad (13)$$

In the current flow in the approximation of the NSF model $p_{yy} = 0$, therefore

$$P_{yy} = \rho RT\,. \qquad (14)$$

Equations (13) and (14) in combination with an obvious ratio

$$\frac{1}{L}\int_0^L \rho\, dy = \rho_0 \qquad (15)$$

allow to determine the density field:

$$\rho = L\rho_0\left(T\int_0^L dy/T\right)^{-1}. \qquad (16)$$

The equation of conservation of momentum, written relative to u_x, and the energy equation of system (6-1) are transformed as

$$\partial P_{xy}/\partial y = 0\,, \qquad (17)$$

$$c_v\left(\gamma-1\right)P_{xy}\partial u_x/\partial y + \partial q_x/\partial y = 0\,. \qquad (18)$$

For the NSF model, boundary slipping conditions of the boundary layer with coefficients obtained in [10] were assumed. The values of the parameter s corresponding to the best agreement with the experimental coefficients of friction on the surface of the plates are taken from the same work.
Testing has shown that the greatest imprecision between the results of different models is observed on the temperature profile. In Fig. 4 the temperature profiles for a weakly nonequilibrium flow are shown. All considered models give almost identical results.

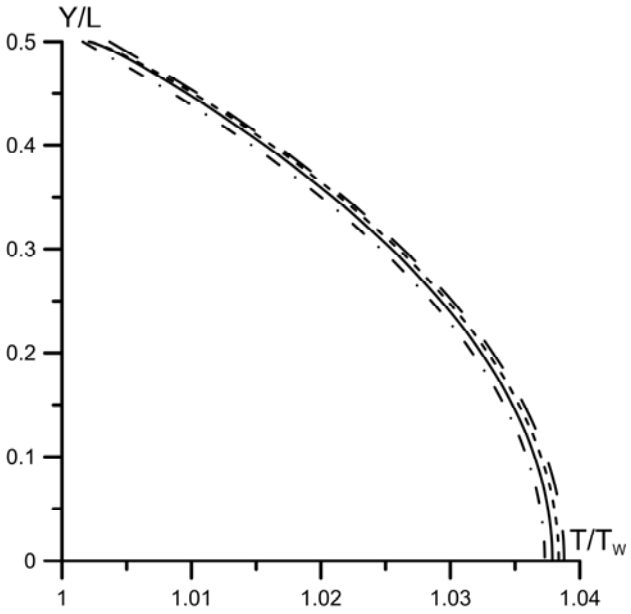

Fig.4. Temperature profiles. $M_\infty = 1$, $Kn = 0.01$. The solid line is a combined model, variant A; fine dotted line is MKE model, large dotted line is NSF model; dash-dotted line is combined model, variant B.

The kinetic subdomain of the composed model A was $2\lambda_0$. The step of the calculated grids of all models was taken constant and made up $0.1\lambda_0$. Only the hydrodynamic grid of the composed model B was plotted in increments λ_0.

Variant B of the composed model required about three times less processor time than variant A. At smaller Kn these advantages of variant B will obviously increase.

A strongly nonequilibrium flow is shown in Fig. 5. The solution of the composed model remains smooth, satisfactorily approximates the kinetic solution, and substantially refines the solution of the NSF model.

In all tests, the solution of the combined model did not contain discontinuities. It should also be noted that in the problem of the Couette flow, shear stresses play a decisive role.

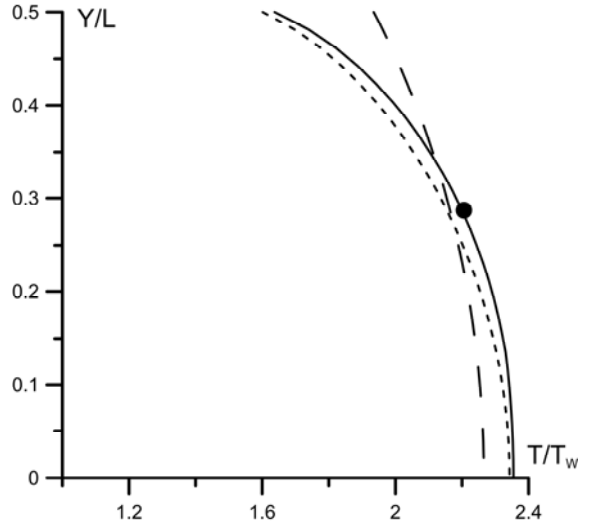

Fig.5. Temperature profiles. $M_\infty = 5$, $Kn = 0.2$. The solid line is a combined model, variant A; fine dotted line is MKE model, large dotted line is NSF model; ● is the boundary point of the kinetic subdomain of the composed model.

5.2 The problem of the structure of the shock wave

The problem is solved in a stationary formulation and is formulated as follows. On the boundaries of the computational domain, the Rankine-Hugoniot conditions are set. The size of the computational domain is several tens of free paths of the molecule in the undisturbed flow:

$$\lambda_\infty = 3.2\mu_\infty \left(2\pi R T_\infty\right)^{-1/2} / \rho_\infty \qquad (19)$$

The system of equations of the *MKE* model is transformed as follows:

$$\xi_x \frac{\partial}{\partial x}\left|\begin{matrix} f_t \\ f_r \end{matrix}\right| = \frac{p}{\mu}\left|\begin{matrix} f_t^+ - f_t \\ f_r^+ - f_r \end{matrix}\right|. \qquad (20)$$

The transformation of the functions and parameters entering into (20) is obvious.

The system of equations of the *NSF* model for this problem:

$$\begin{cases} \rho u_x = \rho_\infty u_{x\infty} \\ \rho u_x \, \partial u_x / \partial x + \partial P_{xx} / \partial x_x = 0 \\ \rho u_x \, \partial T / \partial x + (\gamma - 1) P_{xx} \, \partial u_x / \partial x_x + c_v^{-1} \, \partial q_x / \partial x = 0 \end{cases} \qquad (21)$$

In all calculations, approximations of the viscosity coefficient were taken as $\mu = \mu\left(T_t^s\right)$ for the kinetic model and $\mu = \mu\left(T^s\right)$ for the hydrodynamic one. The power s was chosen from considerations of the best coincidence of the density profile with the experimental profiles of [13, 14]. The parameter Z approximations for various flow regimes are taken from [9, 12, 16]. Difference schemes are as described in Section 4, variant *A*.

The calculated shock wave profiles of the composed model were compared with the profiles of the *MKE* and *NSF* models. Calculations showed that the greatest disarrangement between the profiles of the composed model and the *MKE* model takes place on the temperature profiles. Density and group velocity profiles agreed much better. In the following, only temperature profiles referenced to a single segment T^* will be considered.

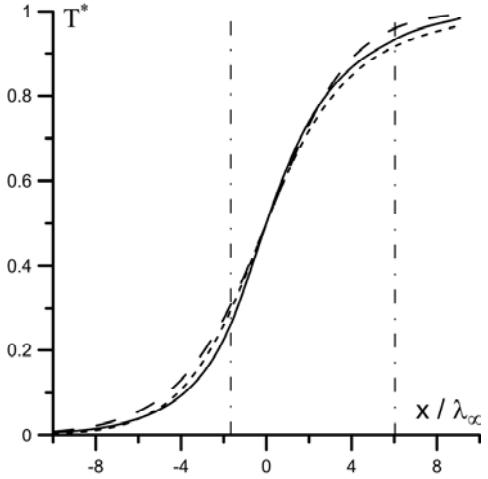

Fig.6. The referenced temperature profiles in a plane shock wave of a diatomic gas. $M_\infty = 1.55$. The solid line is the composed model; fine dotted line is model *MKE*; large dotted line is *NSF* model; vertical dash-dotted lines are the boundaries of the kinetic subdomain of the composed model

In the region of moderate Mach numbers, the composed model produced smooth profiles, although in the kinetic solution subdomain, a noticeable difference was observed from the profiles of the *MKE* model. Fig. 6 shows temperature profiles for $\mathrm{M}_\infty = 1.55$.

The size of the kinetic subdomain of the composed model was $7.8\lambda_\infty$. The joining nodes of the models were in the high gradient subdomain. With an increase in the size of the kinetic subdomain, the corresponding profile became closer to the profile of the *MKE* model. Analysis of the second temperature derivatives at the joining nodes did not reveal a discontinuity of the first derivatives, that is, a break in the graph.

This type of solution was observed until $\mathrm{M}_\infty \approx 2$. For larger Mach numbers, even for sufficiently large sizes of the kinetic subdomain ($20 \div 30\,\lambda_\infty$), a discontinuity of derivatives appeared at its boundary nodes. At the same time, the profile of the kinetic region of the composed model came close to the profile of the *MKE* model.

Fig. 7 shows the temperature profiles in the case of hypersonic flow. In the left boundary node of the kinetic subdomain of the composed model, a pronounced discontinuity of the derivatives is observed. The size of the kinetic subdomain of the composed model is $17.2\,\lambda_\infty$. The profile of the kinetic subdomain of the composed model almost coincides with the profile of the *MKE*.

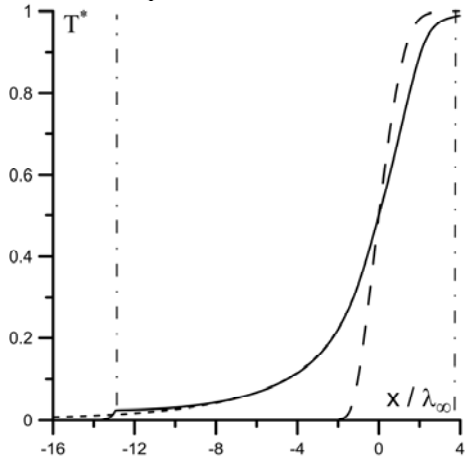

Fig.7. Same as Fig.6, $M_\infty = 7$

Another characteristic feature of the composed model is that throughout the computational domain, including the derivative disontinuity node, the conservation laws are fulfilled up to the error of numerical integration of the weight function over the velocity space.

From Fig. 7 it also follows that despite the discontinuity of the derivative in the boundary node of the kinetic subdomain, the composed model can significantly improve the hydrodynamic solution.

A quantitative estimate of the maximum relative error in calculating the temperature depending on the size of the kinetic region of the combined model is shown in Fig.8.

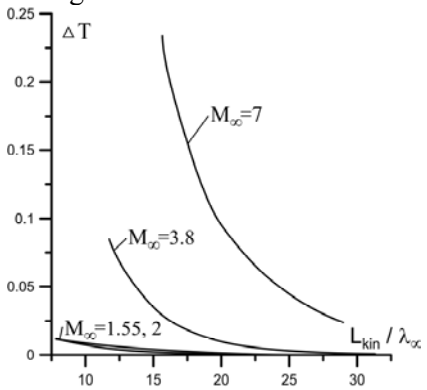

Fig.8. Maximum relative error of temperature calculation depending on the length of the kinetic subdomain of the composed model

6 Conclusion

This paper shows that the composition of a hydrodynamic and kinetic flow models can be quite

successful if both models are based on a single physical model.

By analogy with the proposed model, a composed model can be constructed in which the moment equations of any arbitrarily high order are used to hydrodynamically describe the flow. This removes the question of setting boundary conditions on a solid surface. For all moments included in the system of differential equations, Dirichlet boundary conditions hold.

For practical problems related to the description of flows near solid surfaces, the developed composed model is suitable in the presented form. Apparently, additional development requires only a simple algorithm of transition from one version of the model to another when describing flows in a wide range of Knudsen numbers.

Additional research requires the development of an algorithm to isolate highly non-equilibrium regions in the flow field, for example, the selection of a shock wave front. The upper estimate of the size of the kinetic region of the model in the case of shock waves can serve as data for a plane shock wave presented in Fig.8.

A characteristic feature of the studies performed can be a model effect obtained for highly non-equilibrium flows. As a result of research, it was found that with a small flow nonequilibrium, the kinetic subdomain of the composed model is only slightly, but not significantly different from that of the "pure" kinetic model. In the case of joining a subdomain in the region of high nonequilibrium and the presence, as a consequence, of a discontinuity of the main hydrodynamic functions, the kinetic subdomain almost coincided with the "pure" kinetic solution.

This model effect is not explained by the authors of this paper. Authors will be grateful for comments and useful comments.

References:

[1] P. Degond, S. Jin, L. Mieussens, A smooth transition model between kinetic and hydrodynamic equations, *Journal of Computational Physics*, No.209, 2005, pp. 665–694.

[2] I.V. Egorov, A.I. Erofeev, Continuum and kinetic approaches to the simulation of the hypersonic flow past a flat plate, *Fluid Dynamics*, Volume 32, Issue 1, January 1997, pp 112–122.

[3] G. Abbate, C.R. Kleijn, B.J. Thijsse, Hybrid continuum/molecular simulations of transient gas flows with rarefaction, *AIAA Journal*, Vol. 47, No. 7, 2009, pp. 1741-1749.

[4] N. Crouseilles, P. Degond, M. Lemou, A hybrid kinetic-fluid model for solving the gas dynamics Boltzmann-BGK equations, *J. Comput. Phys.*, 199, 2004, pp 776-808.

[5] N. Crouseilles, P. Degond, M. Lemou, A hybrid kinetic-fluid model for solving the Vlasov-BGK equations, *Journal of Computational Physics*, 203, 2005, pp 572-601.

[6] E.M. Shakhov, *Metod issledovaniia dvizhenii razrezhennogo gaza*, M.: Nauka, 1975. 207 s.

[7] O.I. Rovenskaya, G. Croce, Numerical simulation of gas flow in rough micro channels: hybrid kinetic–continuum approach versus Navier–Stokes, *Microfluid Nanofluid*, 2016, 20:81.

[8] Yu.A. Nikitchenko, Model Kinetic Equation for Polyatomic Gases, *Computational Mathematics and Mathematical Physics*, Volume 57, Issue 11, November 2017, pp 1843–1855.

[9] Yu.A. Nikitchenko, *Modeli neravnovesnykh techenii*, M.: Izd-vo MAI, 2013. 160 s.

[10] V.A. Rykov, A model kinetic equation for a gas with rotational degrees of freedom, *Fluid Dynamics*, Volume 10, Issue 6, November 1975, pp 959–966.

[11] I.N. Larina, V.A. Rykov, Kinetic model of the Boltzmann equation for a diatomic gas with rotational degrees of freedom, *Computational Mathematics and Mathematical Physics*, Volume 50, Issue 12, December 2010, pp 2118–2130

[12] H. Alsmeyer, Density profiles in argon and nitrogen shock waves measured by the absorption of an electron beam, *J. Fluid Mech.*, V. 74, Pt. 3, 1976, pp. 497-513.

[13] F. Robben, L. Talbot, Experimental study of the rotational distribution function of nitrogen in a shock wave, *Phys. Fluids*, V. 9, № 4, 1966, pp. 653-662.

[14] V.S. Glinkina, Yu.A. Nikitchenko, S.A. Popov, Yu.A. Ryzhov, Drag Coefficient of an Absorbing Plate Set Transverse to a Flow, *Fluid Dynamics*, November 2016, Volume 51, Issue 6, pp 791–798.

[15] A.I. Erofeev. Investigation of the Nitrogen Shock Wave Structure on the Basis of Trajectory Calculations of the Molecular Interaction, *Fluid Dynamics*, Volume 37, Issue 6, November 2002, pp 970–982.

[16] Elizarova T.G., Khokhlov A.A., Montero S., Numerical simulation of shock wave structure in nitrogen, *Physics of Fluids*, vol.19 (N 6) 068102, 2007.

[17] M.E. Berezko, Yu.A. Nikitchenko, A.V. Tikhonovets, Sshivanie kineticheskoi i gidrodinamicheskoi modelei na primere techeniya Kuetta, *Trudy MAI*, Vyp.№94, http://trudymai.ru/published.php?ID=80922.